

PAPER • OPEN ACCESS

Fabrication and characterization of the porous titanium alloy by argon filled pore expansion technique

To cite this article: A W Nugroho *et al* 2018 *IOP Conf. Ser.: Mater. Sci. Eng.* **403** 012096

View the [article online](#) for updates and enhancements.



IOP | ebooks™

Bringing you innovative digital publishing with leading voices to create your essential collection of books in STEM research.

Start exploring the collection - download the first chapter of every title for free.

Fabrication and characterization of the porous titanium alloy by argon filled pore expansion technique

A W Nugroho¹, G Leadbeater² and I J Davies²

¹Mechanical Engineering Department, Universitas Muhammadiyah Yogyakarta, Yogyakarta, Indonesia

²Mecahnical Engineering Department Curtin University, Perth, Western Australia, Australia

ariswidyo.nugroho@umy.ac.id .

Abstract. The characterization of fabricated porous β titanium alloy using powder metallurgy technique from elemental powders, i.e. Ti, Nb, Ta and Zr has been carried out. Those elemental powders were blended and filled in steel container. The container was vacuumed and pressurized with argon gas subsequently. The pressurized container was subjected for hot isostatic pressing (HIP-ing) at temperature of 1100°C under 100 MPa of argon pressure subsequent furnace cooling. The HIP-ed container was cut into cubic shape followed by placing in vacuum furnace at high temperatures of 1100°C and 1125°C for foaming process. While microstructure and hardness examination by electron microscope and Vickers indentation were respectively conducted, chemical composition of the porous alloy was determined using X-ray fluorescence (XRF). Their corrosion behavior was evaluated by using potentiodynamic polarization technique. The result shows that whilst the porosity level and the hardness increased with the increase of foaming temperature, the specimen foamed at the lower temperature exhibited higher pitting and corrosion resistance.

1. Introduction

Titanium and its alloys are widely used for many applications because of their advantages such as high specific strength and excellent corrosion resistance. Metal in porous structure demonstrates significant advantages for examples low density and novel acoustic, physical, electrical, thermal, and mechanical properties. Due to high melting point (1670°C) and high reactivity of pure titanium, some fabrication techniques in solid route have referred to produce porous titanium alloys [1-3] compared to the melting route. From those, the argon filled pore expansion technique exhibits no contamination and porosity c.a. 40% in closed pore structure.

Whilst pure titanium powder or prealloyed titanium alloy powder are commonly used as starting material, the use of elemental powder which lowers in cost is rarely reported. Titanium alloying elements: Ti, Zr, Nb and Ta have been reported showing excellent biocompatibility, lowering the Young's modulus and also possessing a considerably superior corrosion resistance. This paper presents the characterization of fabricated porous titanium alloy based on the pressurized argon pore expansion process by powder metallurgy technique using the elemental powders.



2. Methodology

Ti, Nb, Ta and Zr elemental powders in angular shape with the purity and size of the elemental powders being $> 99.5\%$ and $< 44 \mu\text{m}$, respectively were supplied from Cerac Inc. The powders were weighed in accordance to a desired composition of Ti-29Nb-13Ta-4.5Zr, and were then mixed for 30 minutes in a roller bottle mixer at 50 rpm. While figure 1(a) depicts the morphologies of the elemental powders after the mixing process, figure 1(b) presents their energy spectra from Energy Dispersive Spectrometer (EDS) measurement.

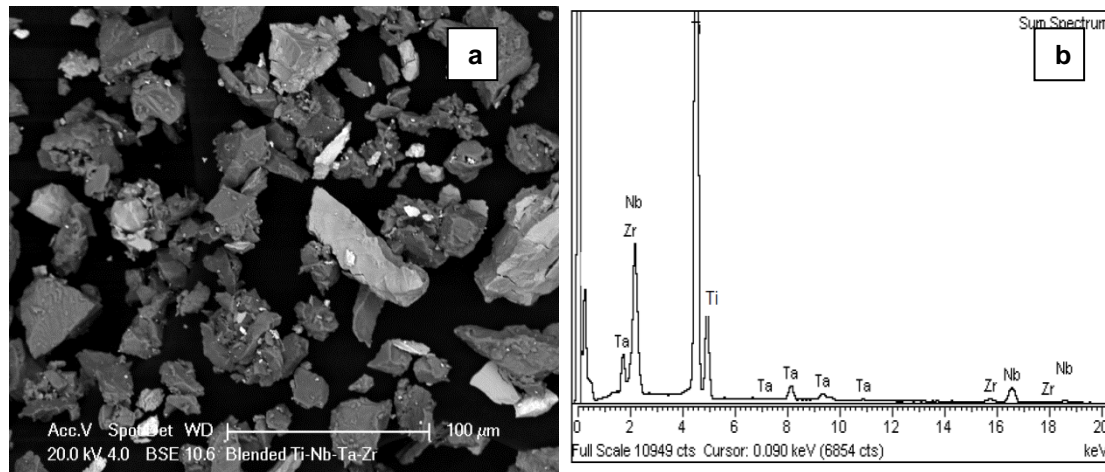


Figure 1. Morphologies of the mixed powder from backscattered scanning electron micrograph (a) the energy spectra from EDS measurement (b).

Afterward, the mixed powder was filled in 30 mm diameter steel containers. The containers were vacuumed and pressurized with argon gas at 0.68 MPa and air tightened by welding subsequently. The pressurized containers were put in hot isostatic press (HIP) machine and heated up at temperature of 1100°C for 1 hours under 100 MPa of argon pressure and slow cooled resulting high pressure argon entrapped in titanium matrix. The HIP-ed billet were cut to cubical shape with dimensions of 10 x 10 x 10 mm by wire electrical discharge machining (WEDM). The cube specimens were then placed in a vacuum furnace for expansion of the pressurized argon or foaming process at 1100° and 1225° for 10 hours. An optical microscopy and an electron microscopy-coupled by EDS were used to examine morphology and microstructure of the prepared foamed specimens. Quantitative analysis of the alloy constituent and fraction porosity were determined using a XRF and open source software digital image analyzer (ImageJ) respectively. Microvickers hardness testing was carried out to reveal hardness values of the porous alloy. Their corrosion behavior was evaluated by open-circuit potential (OCP) and potentiodynamic polarization measurements.

3. Results and discussion

Figure 2 depicted the comparison between a polished HIP-ed specimen and as-foamed specimens before evaluation. The foamed specimens showed darker surface due to pores formed. Generally, the pores expanded in a uniform manner and the extent of pore expansion was determined by the foaming condition. It can be clearly observed that the dimensional changed after foaming process. Foaming at higher temperature appeared in larger side length. This may reflect that porosity level of the foamed specimen at higher temperature (1225°C) is higher than that of the lower one (1100°C).

Barreling shape of the foamed specimen was also noted in which the length of the edge of the foamed specimen was found slightly shorter than that of the middle because of the higher expansion of pressurized argon in metal matrix in the middle. After sectioning by WEDM, surface damage layer of the foamed specimen was removed and polished subsequently. The prepared specimens were then

examined for pore morphology and pore size. The examination area mostly near to the specimen center, otherwise it would be specifically stated.

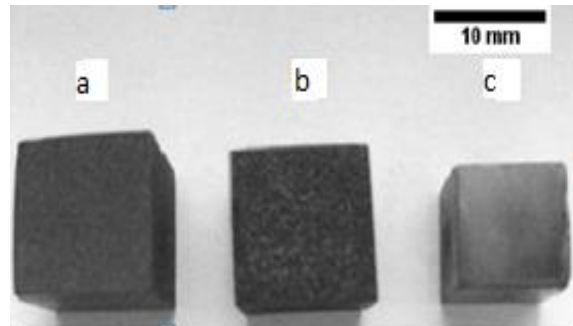
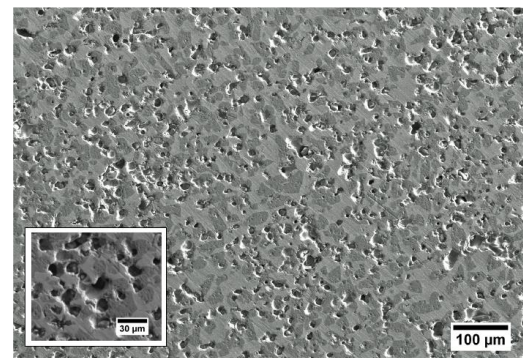
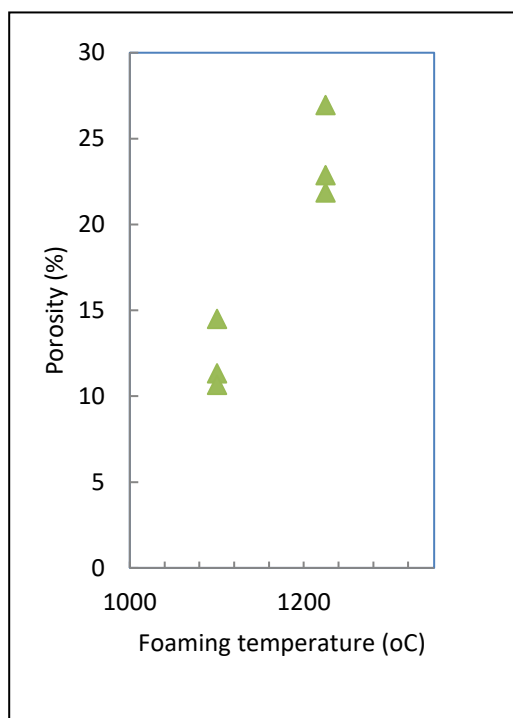
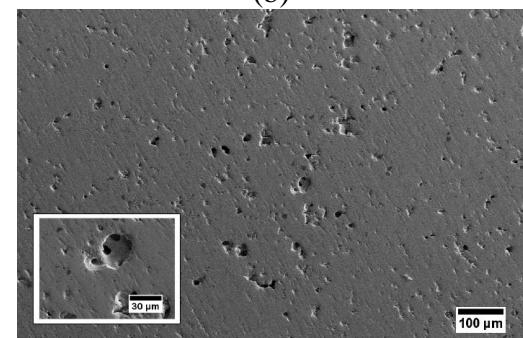


Figure 2. The comparison of foamed titanium alloy specimen at temperature of 1225°C (a), 1100°C (b) and polished HIP-ed billet (c).

The foaming process at 1100°C for 10 hours with pressurized argon gas of 0.68 MPa resulted in porosity level in the range of 10.7-14.5%, while that of 1225°C reached higher porosity level in the range of 21.8-27.0% as shown in figure 3(a).



(b)



(c)

Figure 3. The extent of porosity attained for the specimens being foamed at 1100°C and 1225°C (a), secondary electron microscope image presenting morphology of the pore of a specimen being foamed at 1100°C/0.68 MPa/10 hours with porosity of 10.7% (b) and a specimen being foamed at 1225°C/0.68 MPa/10 hours with porosity of 21.6% (c).

Figure 3(b) shows a typical microstructure depicting pore morphology of a specimen being foamed at 1100°C/0.68 MPa/10 hours. The image also illustrates that a low porosity (10.7%) of porous titanium alloy was obtained by the foaming process. At the porosity level, the pores were distributed

unevenly in the specimen with very small number of pore coalescence and the pores being very discrete.

Equiaxed pore shape was mainly observed with probably in 3 dimensions being spherical in shape as depicted by the inset picture. On the other hand, un spherical pore shape (angular) presumably being formed from the expanded interpowder-spacings were also observed.

The extent of porosity is considered equal to past report researches on other porous titanium alloys which stated the porosity of around 12% [4]. In those researches, porous titanium alloys were developed by means of pre-alloyed master powders heated up at 1200oC and held for 10 hours. The pressurized pores of the specimen foamed at 1225°C expanded more obvious because of the metal matrix creeping resulting in specimen with porosity of 21.6% as illustrated in figure 3(b). Morphology of the pores mostly stayed discrete, with more number of pore coalescence being observable (see the inset) than that of the specimen foamed at 1100°C. The enhancing pore connectivity becomes noticeable as well.

In addition, more uniform pore expansion in specimens being fabricated by foaming temperature at 1225°C was found as appeared in figure 4. Since fewer constrain being present, the pores in the area near to surface of the specimen demonstrated higher expansion level than that of the deeper one resulting a raise in porosity level. Yet, pores with thick in wall and discrete in structure were still observed. The number of pore coalescence just increase very slight. In those regards, the pores were still categorized as closed pores. However, some pores had coalesced and connected to the surface of specimen subsequently escaping pressurized argon gas to the atmosphere (see the arrow in figure 4).

The creep deformation that increase with higher foaming temperature was found to attribute the increase of porosity level. Pore morphologies were confirmed in equiaxed shape and elongated shape because of pore coalescence with in general the pore walls remaining thick and the pore connectivity frequently being visible. Therefore, generally, the foaming temperature clearly affects the extent of porosity of the foamed titanium alloys.

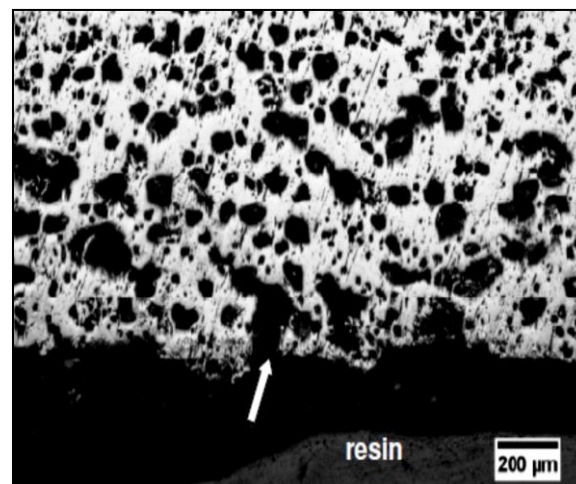


Figure 4. Optical microscope image of the area near to the surface of specimen being foamed at 1225°C showing a relatively uniform pore expansion.

Three specimens were examined by using a XRF to obtain the alloy composition. An XRF spectra of the selected sample is shown in figure 5. The typical chemical composition of Ti, Nb, Ta, Zr and others in the alloy are of $49.6\pm 3.13\%$, $30.6\pm 2.14\%$, $13.47\pm 1.47\%$, $5.97\pm 0.62\%$ and 0.36 ± 0.22 respectively. Whilst this result indicated that the chemical composition of the fabricated alloy is comparable to that of the elemental powders, other elements were detected which may due contamination during alloy processing and samples preparation.

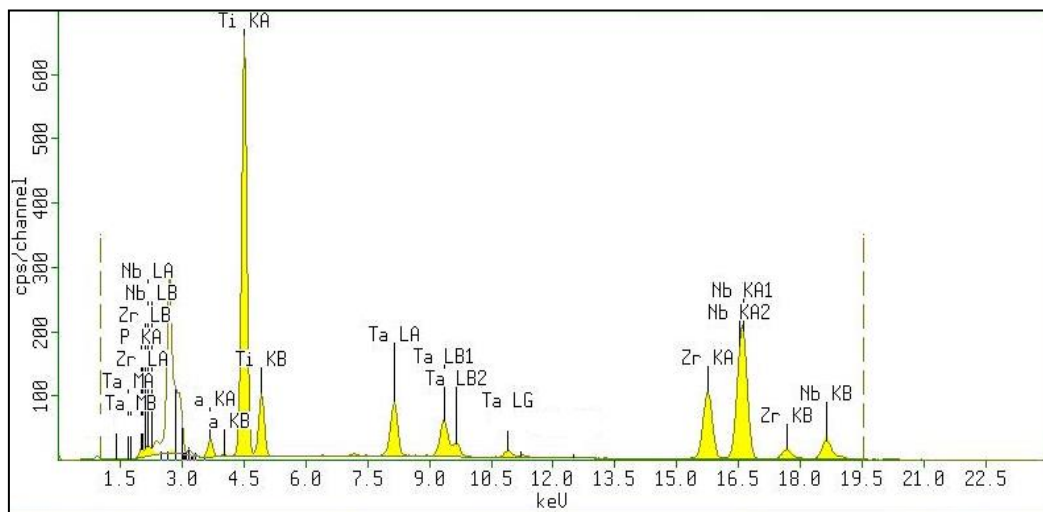


Figure 5. XRF spectra of the titanium alloy.

The hardness testing was conducted on polished specimen surface by means of microvickers hardness testing machine. A load of 100 g was used to carry out the experiment. Figure 6 illustrated the relation between foaming temperature and hardness. Figure 6 presents an increasing foaming temperature increased the hardness.

As expected, the hardness increase with the increase of foaming temperature due to the increase of fraction of α -phase which has higher Young's modulus than that of β -phase as previously revealed [5]. At the higher foaming temperature, fraction of the α -phase rapidly grew rather than that of β -phase resulting in the closer the fraction of the both phases. This allows higher opportunity to obtain individual hardness values of the phases presenting a higher scattered hardness values. In contrast, the specimen being foamed at 1100°C showed a smaller scattered and lower values of hardness value that of at 1225°C. The narrower difference of the hardness for the lower temperature may be suggested by the evident that higher fraction of β -phase was produced by foaming at the lower temperature. Thus, foaming temperature at 1100°C resulted in more homogenous in β -phase than the other. The porous titanium alloy being fabricated consisting of high fraction of β -phase shows hardness which is comparable to the hardness of various biomedical titanium alloys reported in the range of 300-400 HV [6-8].

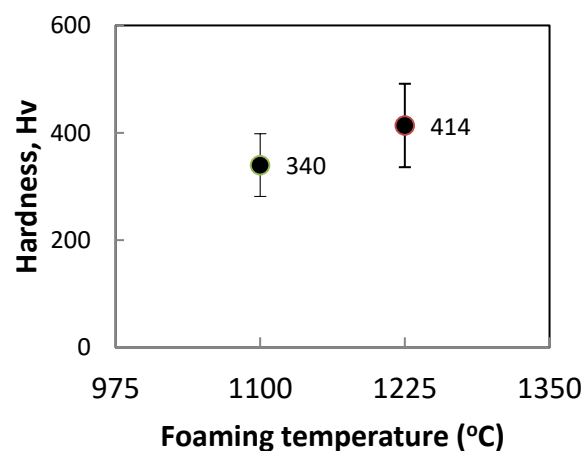


Figure 6. Hardness values of specimen foamed at 1100°C and 1225°C.

In the research, corrosion behavior was assessed using open circuit potential (OCP) method. The OCP measures passivation and layer development of the alloy that occurs in a solution. In addition, potentiodynamic polarization testing was used to identify electrochemical behavior of the material in certain environment. The OCP measurement method's results can be seen in figure 7.

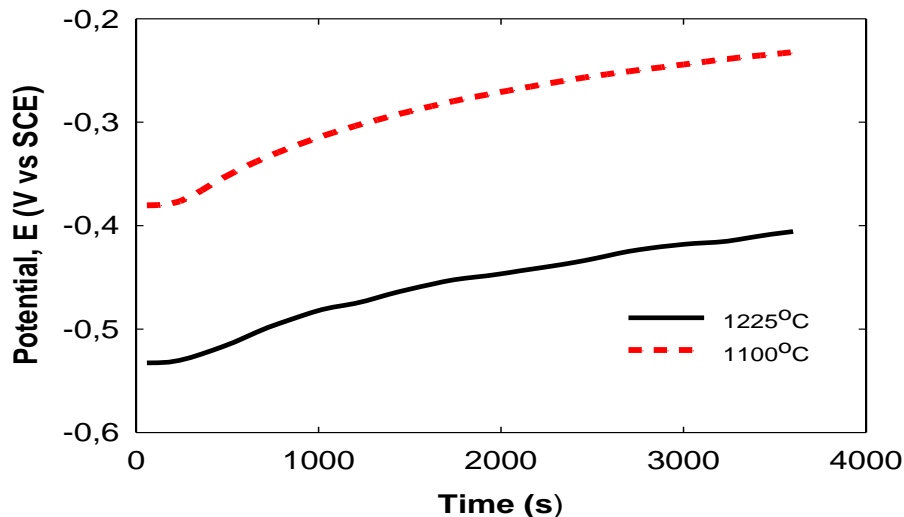


Figure 7. The relation of time to the potential during the OCP measurement in Hank's solution at 37°C of the specimens foamed at 1100°C and 1225°C.

As seen in figure 7, the OCP measurement as a function of time for foaming temperature at 1100°C and 1225°C of the porous alloys. These results can be relatively easy to be reproduced, and all of the curves runs in similar way to each other, in addition to being comparable. Initially, there is a minor upsurge of potential in the first few minutes, followed by a constant rise towards noble direction before becoming steady. The specimen foamed at 1225°C showed the initial E_{corr} of 533 mV. It experienced a moderate increase in increment rate which reached -406 mV after an hour. In addition, the initial corrosion potential (E_{corr}) for the specimen that foamed at 1100°C was found of -380 mV and moderately increase to -232 mV after an hour. The latter specimen had more noble potentials than the former specimen. This increase of potential in the positive way is an indication of a passive film forming, while the steady state implies the film being intact and protective. This signifies a competition between film dissolution and formation, which results in a potential indicating the thickness of surface film and its self-healing properties. The potential variation rate which signifies the formation of oxide was high after a few minutes of immersion, decreasing over time before reaching a steady state.

The potentiodynamic polarization curves for the both foaming temperatures measured in Hank's Solution at 37°C are presented in figure 8. The E_{corr} varied from -445 to -365 mV. This difference among those may be caused by the differing surface condition [9], even though the specimens' preparations used the same procedure.

The corrosion current densities (i_{corr}) were resulted from the polarization's curves by the Tafel extrapolation technique. The breakdown potentials of specimens foamed at 1225°C was of 899 mV. Comparatively, the other specimen which foamed at 1100°C showed neither potential for breakdown nor hysteresis loop (figure 8).

This reveals that the latter specimen has a higher resistance to pitting and crevice corrosion because of its composition, which predominantly comprised the β phase previously reported higher corrosion resistance. In addition, material with higher porosity was also stated susceptibility to crevice corrosion

[10]. Yet, their i_{corr} and E_{corr} in Hank's solution at 37°C could be compared to those of solid CP Ti, Ti 6Al 4V.

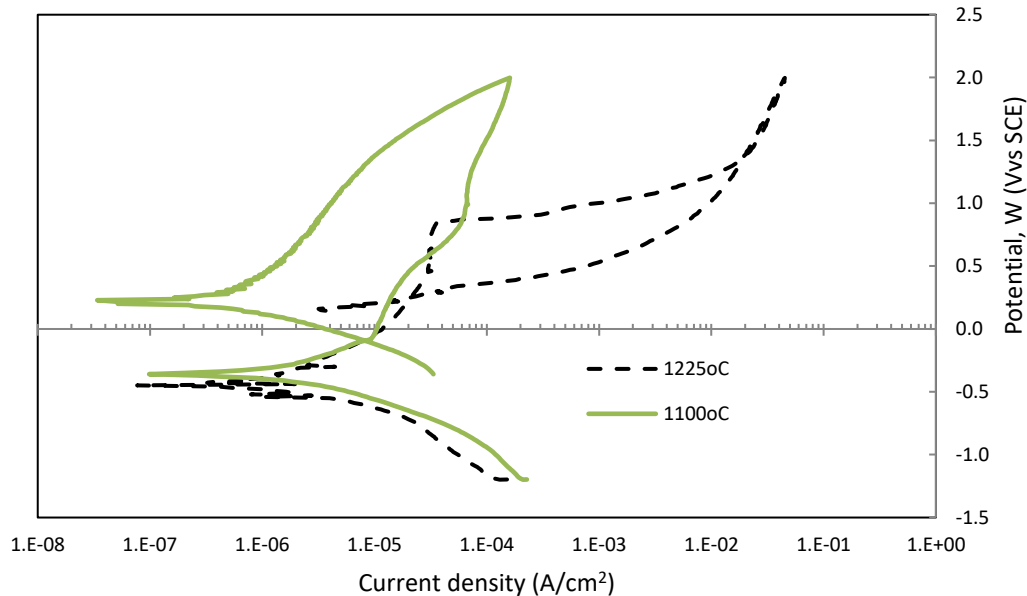


Figure 8. Potentiodynamic polarization curves for specimens foamed at 1100°C and 1225°C in Hank's solution at 37°C.

4. Conclusion

It can be concluded that the porosity level and the hardness increased with the increase of foaming temperature (1100°C and 1225°C) achieving 26.7% and 417mV respectively. The specimen foamed at the lower temperature exhibited higher pitting and corrosion resistance.

References

- [1] Oh I-H, Nomura N, Masahashi N and Hanada S 2003 Mechanical properties of porous titanium compacts prepared by powder sintering *Scripta Materialia* vol 49 issue 12 pp 1197-1202
- [2] Wen C E, Yamada Y and Hodgson P D 2006 Fabrication of novel TiZr alloy foams for biomedical applications *Materials Science and Engineering: C* vol 26 issue 8 pp 1439-44
- [3] Murray N and Dunand D 2006 Effect of initial preform porosity on solid-state foaming of titanium *Journal of Materials Research* vol 21 issue 5 pp 1175-1188
- [4] Oppenheimer S 2007 Processing and characterization of porous Ti-6Al-4V and NiTi *Doctor of Philosophy*, Materials Science and Engineering, Northwestern University, Illinois
- [5] Nugroho A W, Leadbeater G and Davies I J 2011 Processing and properties of porous Ti-Nb-Ta-Zr alloy for biomedical applications using the powder metallurgy route *Australian Journal of Mechanical Engineering* vol 8 issue 2 p 169
- [6] Taddei E B, Henriques V A R, da Silva C R M and Cairo C A A 2007 Age-hardening of Ti-35Nb-7Zr-5Ta alloy for orthopaedic implants *Materials Research* vol 10 no 3 pp 289-92
- [7] Majumdar P, Singh S B and Chakraborty M 2008 Wear response of heat-treated Ti-13Zr-13Nb alloy in dry condition and simulated body fluid *Wear* vol 264 issues 11-12 pp 1015-25
- [8] Niinomi M, Akahori T, Takeuchi T, Katsura S, Fukui H and Toda H 2005 Mechanical properties and cyto-toxicity of new beta type titanium alloy with low melting points for dental applications *Materials Science and Engineering: C* vol 25 issue 3 pp 417-25
- [9] Kim H-K and Jang J-W 2004 Electrochemical corrosion behavior and MG-63 osteoblast-like cell response of surface-treated titanium *Metals and Materials International* vol. 10 issue 5 pp 439-46

- [10] Fojt J, Joska L and Málek J 2013 Corrosion behaviour of porous Ti-39Nb alloy for biomedical application *Corrosion Science* vol 17 pp 78-83